

Hypoxia-Targeted siRNA Delivery**

F. Perche, S. Biswas, T. Wang, L. Zhu, and V. P. Torchilin*

Abstract: Altered vasculature and the resultant chaotic tumor blood flow lead to the appearance in fast-growing tumors of regions with gradients of oxygen tension and acute hypoxia (less than 1.4% oxygen).^[1] Due to its roles in tumorigenesis and resistance to therapy, hypoxia represents a problem in cancer therapy.^[1,2] Insufficient delivery of therapeutic agents to the hypoxic regions in solid tumors is recognized as one of the causes of resistance to therapy.^[1,3] This led to the development of hypoxia imaging agents,^[4] and the use of hypoxia-activated anticancer prodrugs.^[2a] Here we show the first example of the hypoxia-induced siRNA uptake and silencing using a nano-carrier consisting of polyethyleneglycol2000, azobenzene, polyethyleneimine (PEI) (1.8 kDa), and 1,2-dioleoyl-sn-glycero-3-phosphoethanolamine (DOPE) units (the nanocarrier is referred to as PAPD), where azobenzene imparts hypoxia sensitivity and specificity.^[4a] We report hypoxia-activated green fluorescent protein (GFP) silencing in vitro and its down-regulation in GFP-expressing tumors after intravenous administration. The proposed nanoformulation represents a novel tumor-environment-responsive modality for cancer targeting and siRNA delivery.

The specificity and potency of siRNA regulation of gene expression holds great promise for cancer therapy.^[5] However, siRNA delivery to hypoxic regions is challenging since such regions are distant from blood vessels and have increased efflux transporters.^[1] In addition, the use of nano-carriers is required to protect siRNA from degradation and to promote its cellular internalization and endosomal escape.^[5a] Usually, nanoparticle applications rely on the enhanced

permeability and retention (EPR) effect for accumulation in tumor tissue.^[6] Nanoparticles are expected to show preferential extravasation from the circulation when they reach the altered tumor vasculature with its widened endothelial fenestrae and deficient pericyte coverage. Conjugation of polyethyleneglycol (PEG) to nanoparticles extends their blood circulation time, increasing the probability of tumor accumulation by EPR.^[7] However, PEGylation can also hinder cellular uptake resulting in decreased therapeutic activity.^[5a,7a] This PEG dilemma led to the design of nano-formulations with PEG that can be detached upon tumor stimulus to target payload delivery.^[6,8] Nitroimidazole derivatives have been proposed as hypoxia sensors since they are subject to intracellular reduction with formation of free radicals.^[1a,2b,4b] While these free radicals are rapidly oxidized by molecular oxygen, their stabilization under hypoxia leads to reduction-mediated cleavage.^[1b,4a,b,9] Nagano and co-workers demonstrated successful hypoxia imaging in vivo with azobenzene-based probes.^[4a,9] In our study, we used azobenzene as a hypoxia-responsive bioreductive linker for hypoxia-targeted delivery of siRNA from PEGylated nanopreparations upon PEG removal/cleavage. The production of GFP was used as a model to test for siRNA downregulation in both in vitro and in vivo studies.

The potency of the azobenzene unit for siRNA delivery was evaluated by linking azobenzene to PEG2000 at one end and to a PEI(1.8 kDa)-DOPE conjugate on the other end to obtain PAPD (Figure 1 a).

PEG2000 was used as the hydrophilic block and for imparting stability in circulation.^[8b,10] The PEI-DOPE conjugate was introduced for siRNA complexation and to promote formation of micellar nanoparticles.^[11] The hypoxia-sensitive polymer PAPD and its insensitive PEG-PEI-DOPE (PPD) counterpart were synthesized (Figures S1-S6) and expected to condense siRNA into nanoparticles with a PEG layer to protect it from the nuclease attack and impart stability in physiological fluids (Figure 1 b).^[7b,8d,10] The PEG groups would be detached from PAPD/siRNA complexes in the hypoxic and reductive^[1b,12] tumor environment because of degradation of the azobenzene linker; as a result PEI's positive charge would be exposed and the remaining PEI-DOPE/siRNA complexes would be taken up in the cell.^[2c,8e,11b]

Formation of complexes between PAPD and siRNA was demonstrated by an ethidium bromide (EtBr) exclusion assay and transmission electron microscopy (Figure 2 a,d). In line with previous results,^[13] a higher N/P ratio of PAPD over PEI was required to quench siRNA fluorescence (16 and 4, respectively). Complexes protected siRNA against RNase degradation (Figure 2 b) and demonstrated moderate unpacking (30% increase in EtBr fluorescence, Figure 2 c) after


[*] Dr. F. Perche,^[+] Dr. T. Wang, Dr. L. Zhu, Prof. V. P. Torchilin
Department of Pharmaceutical Sciences
Bouve College of Health Sciences, Center for Pharmaceutical
Biotechnology and Nanomedicine, Northeastern University
140 The Fenway, Room 230, 360 Huntington Avenue
Boston, MA 02115 (USA)
E-mail: v.torchilin@neu.edu

Dr. S. Biswas^[+]
Birla Institute of Technology & Science-Pilani
Hyderabad Campus
Jawahar Nagar, Shameerpet Mandal, A.P - 500078 (India)

Dr. L. Zhu
Irma Lerma Rangel College of Pharmacy
Texas A&M University Health Science Center
Kingsville, TX 78363 (USA)

[+] These authors contributed equally and should be considered first authors.

[**] This work was supported by grant U54CA151881 to V.P.T. We are grateful to Prof. Mansoor M. Amiji for providing access to the Kodak Imager and William Fowle for transmission electron microscopy.

 Supporting information for this article is available on the WWW under <http://dx.doi.org/10.1002/anie.201308368>.

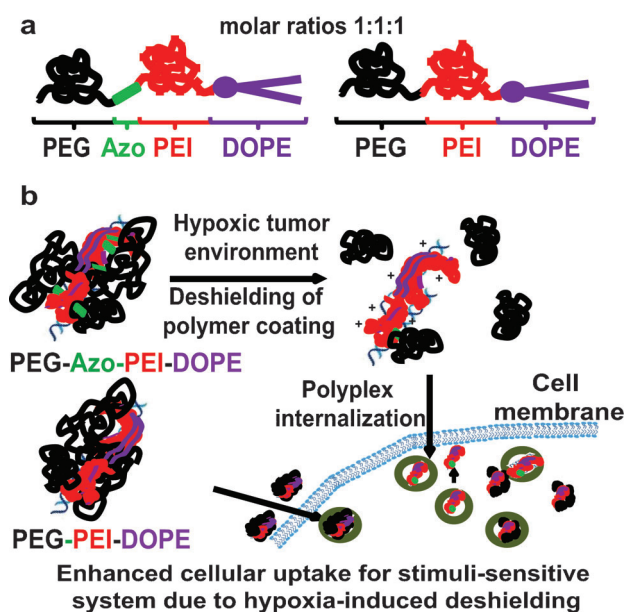


Figure 1. a) Schematic representation of the synthesized polymers and b) proposed mechanism of internalization in hypoxic tumor micro-environment.

incubation in the medium containing 10 % fetal bovine serum, in agreement with Refs. [7b,8e,13,14].

Since reductase-rich rat liver microsomes were reported to cleave nitroimidazole derivatives under hypoxia,^[4a,b,9] we evaluated siRNA condensation and uptake of the complexes after incubation with rat liver microsomes (Figure 2c, Figure 3). While siRNA fluorescence was quenched in PBS (26 % of siRNA fluorescence), the incubation with microsomes led to a threefold increase in fluorescence (Figure 2c) and a threefold increase in aniline absorbance (Figure S8), supporting bioreductive cleavage.^[4b,12] Addition of microsomes also led to a considerable positive charge increase from (0.1 ± 6.5) mV to (13.2 ± 3.7) mV ($p = 0.006$, Student's *t* test) (Figure 2e,f). Exposure of positive surface charges from the siRNA complexes, which were previously hidden by PEG, under reductive hypoxia conditions indicates PEG detachment after azobenzene cleavage.^[2c,4a,8a] By contrast, no such charge exposure was observed for PPD/siRNA complexes (Figure S9). No cytotoxicity was detected after the cells were treated with PPD and PAPD both free and complexed with siRNA and both in normoxic and hypoxic conditions (Figures S10 and S11).

We studied the uptake of the nanopreparations with monolayer cultures of cancer cells in normoxic and hypoxic environments. In vitro hypoxia was confirmed by Hydroxyprobe staining (Figure S12).^[4c] Cellular internalization of PPD or PAPD complexes prepared with Fluorescein amidite (FAM)-labeled siRNA was determined by flow cytometry (Figure 3a,b). The cell-associated fluorescence of PAPD/siRNA-treated cells under hypoxia was 3.2-fold higher than under normoxia (13.4 and 4.1, respectively; Figure 3b) and 3.9-fold higher than for PPD/siRNA under hypoxia.

Cancer cell spheroids have been proposed as models for the evaluation of nanomedicines,^[15] and we used a spheroid

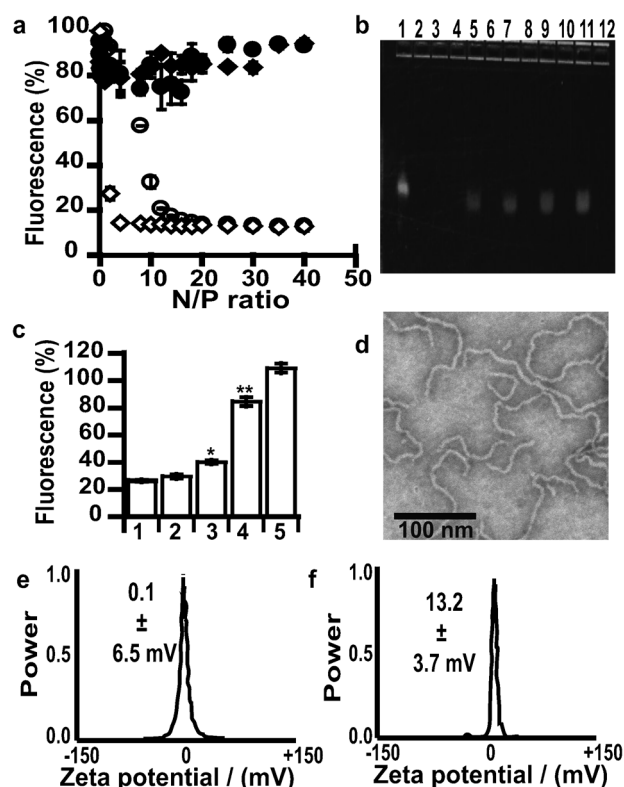


Figure 2. siRNA binding and cytotoxicity. a) Ethidium bromide exclusion assay: PEI 1.8 kDa (\diamond), PAPD (\circ), PEI (1.8 kDa) polyplexes treated with heparin (\blacklozenge), PAPD treated with heparin (\bullet). b) RNAse protection assay. 1. untreated free siRNA; 2. RNAse-treated free siRNA; 4. PAPD polyplexes, N/P 40; 5. PAPD polyplexes, N/P 40 treated with RNAse and heparin; 6. PAPD polyplexes, N/P 60; 7. PAPD polyplexes, N/P 60 treated with RNAse and heparin; 8. PEG-PEI-DOPE (PPD) polyplexes, N/P 40; 9. PPD polyplexes, N/P 40 treated with RNAse and heparin; 10. PPD polyplexes, N/P 60; 11. PPD polyplexes, N/P 60 treated with RNAse and heparin; wells 3 and 12 were unused. c) siRNA signal from PAPD polyplexes prepared at an N/P ratio of 40 and incubated 2 h in 1. PBS, 2. 0 % FBS media, 3. 10 % FBS N_2 -bubbled media, 4. 10 % FBS N_2 -bubbled media and microsomes, 5. PBS followed by heparin treatment; * $p < 0.05$, ** $p < 0.01$ compared with PBS. d) Transmission electron microscopy micrograph of PAPD polyplexes in PBS showing a rodlike structure; scale bar represents 100 nm. e, f) Zeta potential of PAPD/siRNA complexes prepared at an N/P of 40 after incubation with PBS (e) and N_2 -bubbled PBS containing microsomes (f).

model to confirm hypoxia-activated siRNA internalization. Whereas free FAM-siRNA fluorescence was bound to the surface of the spheroids, complexation with PAPD or PPD nanocarriers increased its penetration under normoxia, although only to the first cell layers (Figure 3, Figure S13), as reported by Wong et al. with siRNA lipoplexes.^[16] Only treatment of spheroids with PAPD/siRNA under hypoxia (Figure 3e, Figure S13) resulted in further increase of siRNA penetration. This was matched with a deeper penetration of rhodamine-labeled PEG-Azo-Rhodamine-PEI-DOPE (PARPD) over PEG-Rhodamine-PEI-DOPE (PRPD) (Figure S14). Altogether, this data suggests better uptake of the nanoformulation after PEG deshielding.^[2c,8a,d,e]

We used HeLa cells stably expressing GFP (HeLa/GFP) and some other cells to confirm the PAPD-mediated gene

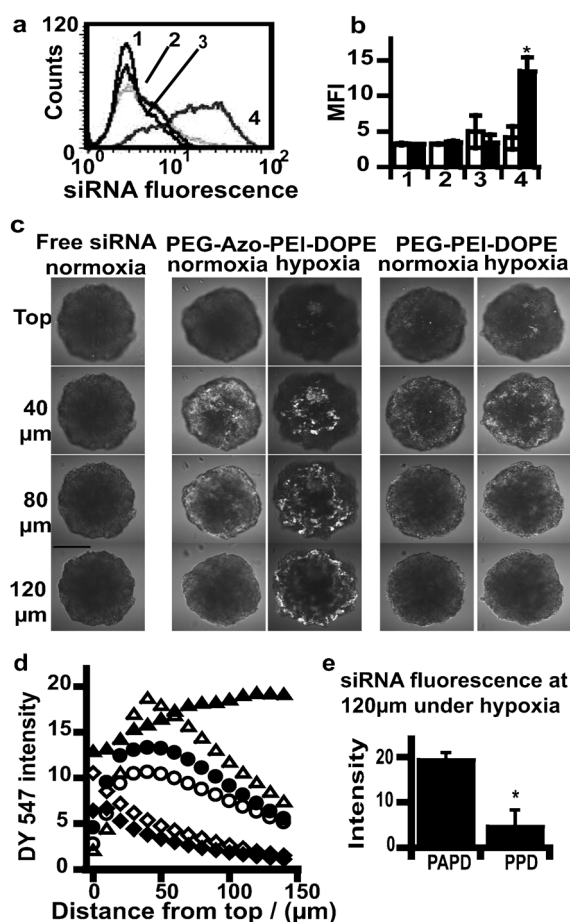


Figure 3. Internalization of siRNA in monolayers and distribution in spheroids. Monolayers: a) Representative histogram plots of cellular internalization under hypoxia in the presence of 10% FBS; 1: PBS-treated cells, 2: free FAM-siRNA, 3: PEG-PEI-DOPE/siRNA, 4: PEG-Azo-PEI-DOPE/siRNA. b) Geometric mean of fluorescence of A549 cells incubated 24 h with the same formulations as in (a) under normoxia (white bars) and hypoxia (black bars). Spheroids: NCI-ADR-RES spheroids were incubated 4 h under normoxia and hypoxia with DY 547-labeled siRNA. c) Imaging of siRNA distribution by confocal microscopy; scale bar represents 250 μm . d) Quantitation of DY 547 fluorescence from the spheroid surface after incubation with free siRNA (\diamond for normoxia, \blacklozenge for hypoxia), PEG-Azo-PEI-DOPE/siRNA (\triangle for normoxia, \blacktriangle for hypoxia) and PEG-PEI-DOPE/siRNA (\circ for normoxia, \bullet for hypoxia). e) Average intensity of fluorescence at 120 μm from spheroid surface after treatment with PEG-Azo-PEI-DOPE/siRNA (PAPD) and PEG-PEI-DOPE/siRNA (PPD) under hypoxia. * $p < 0.05$ compared with PAPD/DY 547 siRNA complexes.

downregulation in the presence of 10% FBS (Figure 4, Figure S15). Whereas no GFP downregulation was observed with PAPD-complexed siRNA under normoxia (Figure 4a), 30–40% downregulation was detected under hypoxia in all HeLa/GFP, NCI-ADR-RES/GFP, and A2780/GFP cells (Figure 4a, Figure S16); there was no significant downregulation when insensitive PPD/siRNA polyplexes were used (Figure 4b). This silencing activity is comparable with that reported earlier using 200 nm siRNA.^[16] Hypoxia-induced silencing was concordant with the internalization results (Figure 3). The silencing activity observed in vitro, which was moderate compared to that associated with Lipofectamine-

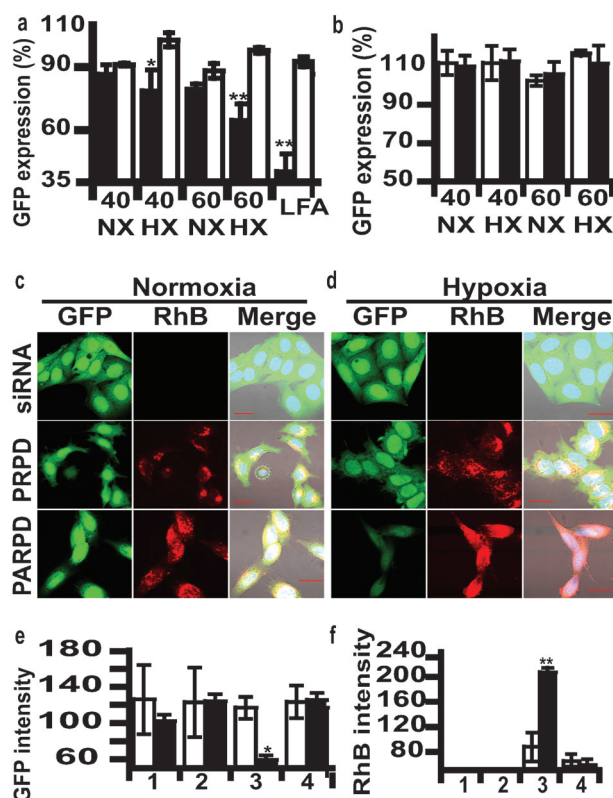


Figure 4. GFP downregulation in vitro. GFP downregulation was evaluated both by flow cytometry (a,b) and microscopy (c–f) after transfection under normoxic (NX) or hypoxic (HX) conditions. Relative geometric mean fluorescence from FACS analysis of HeLa/GFP cells transfected with a) PEG-Azo-PEI-DOPE (PAPD)/siRNA complexes, b) PEG-PEI-DOPE (PPD)/siRNA complexes in the presence of 10% FBS. Polyplexes were prepared at N/P ratios of 40 and 60 with anti-GFP siRNA (black bars) or scrambled siRNA (white bars). Lipofectamine 2000 (LFA) was used as a positive control, * $p < 0.05$, ** $p < 0.01$ compared with scrambled siRNA complexes. CLSM images of HeLa/GFP cells transfected with Rhodamine B labeled copolymers PEG-Azo-Rhodamine-PEI-DOPE (PARPD), PEG-Rhodamine-PEI-DOPE (PRPD) and GFP siRNA under normoxia (c) and hypoxia (d). Mean pixel intensities of GFP (e) and Rhodamine B (f) after transfection under normoxia (white bars) and hypoxia (black bars); 1: PBS, 2: free siRNA, 3: PARPD, 4: PRPD. * $p < 0.05$, ** $p < 0.01$ compared with normoxia.

mediated delivery, may be attributed to incomplete cleavage of the azobenzene unit within the observation time; however, one has to note that the silencing of Lipofectamine complexes is identical under both normoxia and hypoxia, which clearly supports the hypoxic selectivity of our nanocarrier. To corroborate downregulation in hypoxic conditions with internalization, we formed polyplexes using Rhodamine B labeled copolymers (Figure 4c–f). Stronger GFP downregulation under hypoxia over normoxia was proportional to the enhanced PARPD uptake (Figure 4c,d) while an opposite correlation was observed for PRPD (Figure 4d–f).

We then performed a tumor accumulation study of the copolymers 4 h after intravenous administration of PARPD and PRPD to mice bearing hypoxic B16F10 tumors^[3] (Figures S12 and S17–19). A twofold increase in tumor-cell-associated fluorescence intensity was observed only for

PARPD (Figure S17). Fluorescence from polymers was also detected in the blood-filtering organs liver, spleen, and kidney (Figures S17 and S18), off-target sites for nanomedicines.^[2c,5a] Whereas PARPD was detected in tumor sections, PRPD was not found to accumulate in tumors. The data support tumor hypoxia-induced PEG shedding with subsequent PARPD uptake upon the charge exposure, in good agreement with reports on tumor-specific charge exposure.^[2c,8a,d,e]

We finally assessed the ability of GFP silencing in vivo on A2780/GFP tumors in mice (Figure 5). Substantial GFP downregulation was detected after intravenous injection of PAPD/siRNA nanoparticles both by ex vivo imaging (Figure 5a, 24 %) and by flow cytometry (Figure 5b, 32 %). No downregulation was observed with PAPD complexes formed with scrambled siRNA (Figure 5). The in vivo silencing capacity of PAPD corresponded well to its in vitro uptake and silencing profiles (Figures 3 and 4; Figure S15) and tumor accumulation (Figures S17 and S18).

The PAPD nanocarrier has the following attributes: a) PEG for stability in physiological fluids and increased tumor accumulation^[6,10] (Figure 2, Figure S17), b) PEI-DOPE for siRNA complexation, protection from RNase degradation, and endosomal escape^[8e,11b,c] (Figure 2), c) an azobenzene linker for hypoxia-activated charge exposure^[2b,4b,8a,11a,13,16] (Figure 2; Figure S8) to allow d) hypoxia-dependent cellular uptake and accumulation of the copolymer in the tumor cells (Figure 5, Figure S18), and GFP silencing in vivo after intravenous administration (Figure 5) without detectable cytotoxicity (Figures S10, S11, and S20).

Few examples of hypoxia-targeted delivery have been reported.^[2b,c] Our study is, to the best of our knowledge, the

first of its kind with a hypoxia-activated siRNA nanocarrier achieving silencing in vivo. The low oxygen threshold (0.1–1 %) of the azobenzene-based probe described by Kiyose et al.^[4a] suggests the biosafety of PAPD since the side effects associated with tirapazamine were attributed to its high hypoxic activation threshold.^[2a] However, we only detected a moderate silencing activity in vitro and in vivo indicating that the structure should be optimized. We suggest two approaches for further improvement: on the one hand, a compromise between tumor hypoxia activation and cellular uptake by optimization of the chemical structure as in the report by Piao et al.^[9] on the other hand, mixed micelles of PAPD and another copolymer could be prepared for improved silencing activity.^[17] Finally, since hypoxia is one of the characteristics of drug-resistant cancers,^[1] hypoxia-targeted co-delivery of a chemotherapeutic drug and siRNA against the hypoxia principal effector, hypoxia inducible factor 1 α , could allow relapse-free destruction of some of the most aggressive tumors.

Received: September 25, 2013

Published online: February 19, 2014

Keywords: cancer · antitumor agents · hypoxia-triggered copolymer · siRNA delivery · tumor targeting

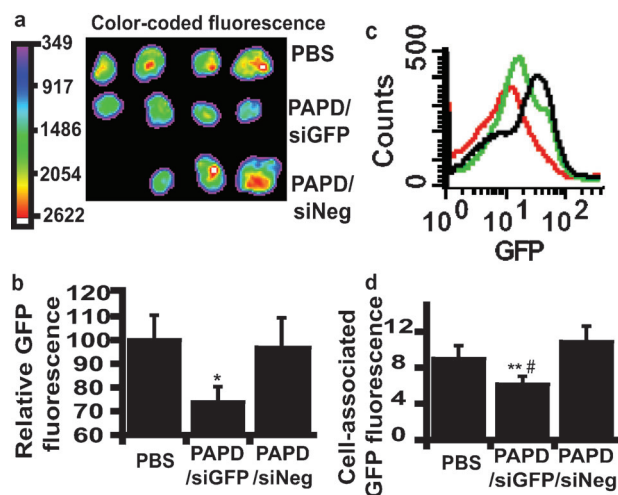


Figure 5. In vivo silencing activity. a) Ex vivo fluorescence optical imaging of tumors 48 h after intravenous injection of PBS ($n=4$), PEG-Azo-PEI-DOPE/anti-GFP siRNA complexes prepared with (PAPD/siGFP, $n=4$), PEG-Azo-PEI-DOPE/negative siRNA complexes (PAPD/siNeg, $n=3$) at a dose of 1.5 mg kg^{-1} of siRNA in $200 \mu\text{L}$ PBS. b) Relative GFP fluorescence from tumors. Student's t test was performed, $*p < 0.05$ compared to PBS or PAPD/siNeg. c) Cell-associated fluorescence of dissociated tumors by flow cytometry and representative histogram (d). Green: PBS, red: PAPD/siGFP, black: PAPD/siNeg. Only PAPD/siGFP led to a significant decrease of GFP expression (Student's t test, $**p < 0.01$ compared to PBS, $\#p < 0.001$ compared to PAPD/siNeg).

- 1) a) J. M. Brown, W. R. Wilson, *Nat. Rev. Cancer* **2004**, *4*, 437–447; b) W. R. Wilson, M. P. Hay, *Nat. Rev. Cancer* **2011**, *11*, 393–410.
- 2) a) J. Kling, *Nat. Biotechnol.* **2012**, *30*, 381; b) Q. Lin, C. Bao, Y. Yang, Q. Liang, D. Zhang, S. Cheng, L. Zhu, *Adv. Mater.* **2013**, *25*, 1981–1986; c) Z. Poon, D. Chang, X. Zhao, P. T. Hammond, *ACS Nano* **2011**, *5*, 4284–4292.
- 3) C. Kieda, B. El Hafny-Rahbi, G. Collet, N. Lamerant-Fayel, C. Grillon, A. Guichard, J. Dulak, A. Jozkowicz, J. Kotlinowski, K. C. Fylaktakidou, A. Vidal, P. Auzeloux, E. Miot-Noirault, J. C. Beloeil, J. M. Lehn, C. Nicolau, *J. Mol. Med.* **2013**, *91*, 883–899.
- 4) a) K. Kiyose, K. Hanaoka, D. Oushiki, T. Nakamura, M. Kajimura, M. Suematsu, H. Nishimatsu, T. Yamane, T. Terai, Y. Hirata, T. Nagano, *J. Am. Chem. Soc.* **2010**, *132*, 15846–15848; b) S. Kizaka-Kondoh, H. Konse-Nagasawa, *Cancer Sci.* **2009**, *100*, 1366–1373; c) K. A. Krohn, J. M. Link, R. P. Mason, *J. Nucl. Med.* **2008**, *49*, 129S–148S.
- 5) a) L. Huang, Y. Liu, *Annu. Rev. Biomed. Eng.* **2011**, *13*, 507–530; b) D. H. Kim, J. J. Rossi, *Nat. Rev. Genet.* **2007**, *8*, 173–184; c) G. J. Weiss, J. Chao, J. D. Neidhart, R. K. Ramanathan, D. Bassett, J. A. Neidhart, C. H. Choi, W. Chow, V. Chung, S. J. Forman, E. Garmey, J. Hwang, D. L. Kalinoski, M. Koczywas, J. Longmate, R. J. Melton, R. Morgan, J. Oliver, J. J. Peterkin, J. L. Ryan, T. Schluep, T. W. Synold, P. Twardowski, M. E. Davis, Y. Yen, *Invest. New Drugs* **2013**, *31*, 986–1000.
- 6) H. Maeda, H. Nakamura, J. Fang, *Adv. Drug Delivery Rev.* **2013**, *65*, 71–79.
- 7) a) Y. H. Bae, K. Park, *J. Controlled Release* **2011**, *153*, 198–205; b) M. Ogris, S. Brunner, S. Schuller, R. Kircheis, E. Wagner, *Gene Ther.* **1999**, *6*, 595–605.
- 8) a) J. J. Li, Z. S. Ge, S. Y. Liu, *Chem. Commun.* **2013**, *49*, 6974–6976; b) H. Hatakeyama, H. Akita, K. Kogure, M. Oishi, Y. Nagasaki, Y. Kihira, M. Ueno, H. Kobayashi, H. Kikuchi, H. Harashima, *Gene Ther.* **2007**, *14*, 68–77; c) T. Ishida, M. J. Kirchmeier, E. H. Moase, S. Zalipsky, T. M. Allen, *Biochim. Biophys. Acta Biomembr.* **2001**, *1515*, 144–158; d) S. Takae, K.

- Miyata, M. Oba, T. Ishii, N. Nishiyama, K. Itaka, Y. Yamasaki, H. Koyama, K. Kataoka, *J. Am. Chem. Soc.* **2008**, *130*, 6001–6009; e) X. Z. Yang, J. Z. Du, S. Dou, C. Q. Mao, H. Y. Long, J. Wang, *ACS Nano* **2012**, *6*, 771–781.
- [9] W. Piao, S. Tsuda, Y. Tanaka, S. Maeda, F. Liu, S. Takahashi, Y. Kushida, T. Komatsu, T. Ueno, T. Terai, T. Nakazawa, M. Uchiyama, K. Morokuma, T. Nagano, K. Hanaoka, *Angew. Chem.* **2013**, *125*, 13266–13270; *Angew. Chem. Int. Ed.* **2013**, *52*, 13028–13032.
- [10] A. L. Klibanov, K. Maruyama, A. M. Beckerleg, V. P. Torchilin, L. Huang, *Biochim. Biophys. Acta Biomembr.* **1991**, *1062*, 142–148.
- [11] a) G. Navarro, R. R. Sawant, S. Biswas, S. Essex, C. Tros de Ilarduya, V. P. Torchilin, *Nanomedicine* **2012**, *7*, 65–78; b) R. R. Sawant, S. K. Sriraman, G. Navarro, S. Biswas, R. A. Dalvi, V. P. Torchilin, *Biomaterials* **2012**, *33*, 3942–3951; c) G. Navarro, S. Essex, R. R. Sawant, S. Biswas, D. Nagesha, S. Sridhar, C. T. de Ilarduya, V. P. Torchilin, *Nanomedicine: Nanotechnology, Biology and Medicine* **2013**.
- [12] H. JooáJung, T. GeoláLee, T. DongáChung, *Chem. Commun.* **2010**, *46*, 3863–3865.
- [13] A. Malek, F. Czubyko, A. Aigner, *J. Drug Targeting* **2008**, *16*, 124–139.
- [14] R. S. Burke, S. H. Pun, *Bioconjugate Chem.* **2008**, *19*, 693–704.
- [15] G. Mehta, A. Y. Hsiao, M. Ingram, G. D. Luker, S. Takayama, *J. Controlled Release* **2012**, *164*, 192–204.
- [16] H. L. Wong, Z. Shen, Z. Lu, M. G. Wientjes, J. L. Au, *Mol. Pharm.* **2011**, *8*, 833–840.
- [17] M. Omedes Pujol, D. J. Coleman, C. D. Allen, O. Heidenreich, D. A. Fulton, *J. Controlled Release* **2013**, *172*, 939–945.